3634–3642 *Nucleic Acids Research, 2017, Vol. 45, No. 7* *Published online 15 March 2017*
doi: 10.1093/nar/gkx171

Iron mediates catalysis of nucleic acid processing enzymes: support for Fe(II) as a cofactor before the great oxidation event

C. Denise Okafor, Kathryn A. Lanier, Anton S. Petrov, Shreyas S. Athavale, Jessica C. Bowman, Nicholas V. Hud and Loren Dean Williams*

School of Chemistry and Biochemistry, Georgia Institute of Technology, Atlanta, GA 30332 0400, USA

Received October 05, 2016; Revised February 27, 2017; Editorial Decision February 28, 2017; Accepted March 08, 2017

ABSTRACT

Life originated in an anoxic, Fe^{2+}-rich environment. We hypothesize that on early Earth, Fe^{2+} was a ubiquitous cofactor for nucleic acids, with roles in RNA folding and catalysis as well as in processing of nucleic acids by protein enzymes. In this model, Mg^{2+} replaced Fe^{2+} as the primary cofactor for nucleic acids in parallel with known metal substitutions of metalloproteins, driven by the Great Oxidation Event. To test predictions of this model, we assay the ability of nucleic acid processing enzymes, including a DNA polymerase, an RNA polymerase and a DNA ligase, to use Fe^{2+} in place of Mg^{2+} as a cofactor during catalysis. Results show that Fe^{2+} can indeed substitute for Mg^{2+} in catalytic function of these enzymes. Additionally, we use calculations to unravel differences in energetics, structures and reactivities of relevant Mg^{2+} and Fe^{2+} complexes. Computation explains why Fe^{2+} can be a more potent cofactor than Mg^{2+} in a variety of folding and catalytic functions. We propose that the rise of O_2 on Earth drove a Fe^{2+} to Mg^{2+} substitution in proteins and nucleic acids, a hypothesis consistent with a general model in which some modern biochemical systems retain latent abilities to revert to primordial Fe^{2+}-based states when exposed to pre-GOE conditions.

INTRODUCTION

Iron was abundant, benign and soluble when life originated on the ancient earth (1–5). The geological record indicates that for ∼2 billion years the oceans contained vast quantities of soluble Fe^{2+}, with concentrations on the order of 10^{-4} M. The reducing conditions of the ancient Earth favored Fe^{2+} over Fe^{3+} and mitigated destructive iron-mediated processes such as Fenton chemistry (6,7). During the first half of Earth's history iron became broadly involved in protein-mediated biochemistry (8,9). The wide distribution of iron in extant biological systems (10), despite its harmful effects and low solubility on the surface of the extant Earth, highlights this element's catalytic utility and deep evolutionary history.

Approximately 2 billion years ago, O_2 began accumulating in the atmosphere, triggering global shifts in biochemistry and microbiology. This Great Oxidation Event (GOE) brought the modern condition of iron scarcity (10^{-9} M in the oceans) and iron-mediated oxidative damage to biological systems (11). The GOE drove substitution of copper, zinc, manganese and other metals for iron in metabolic enzymes (8,12–18) as well as tight regulation of cellular distributions and concentrations (10).

We hypothesize that on the ancient earth, Fe^{2+} was a primary divalent cofactor in protein-based nucleic acid processing enzymes as well as in ribozymes (23,24). In this model, the GOE drove biosphere-wide $Fe^{2+} \rightarrow Mg^{2+}$ substitutions in both enzymes and ribozymes. The abilities of these two metals to substitute for each other are consistent with similarities in their coordination chemistries (Table 1). An earth-wide $Fe^{2+} \rightarrow Mg^{2+}$ substitution in nucleic acid processing enzymes and in ribozymes has analogy to well-established substitutions of Cu^{2+}, Zn^{2+}, Mn^{2+} for Fe^{2+} in metabolic enzymes (8,12–18). In our $Fe^{2+} \rightarrow Mg^{2+}$ model, the early emergence of polymerases, ligases, nucleases, repair enzymes and ribozymes was facilitated by interactions with Fe^{2+}.

Magnesium seems to be essential for function of extant DNA polymerases, RNA polymerases and DNA ligases. A consensus of data supports a two divalent metal cation mechanism of phosphoryl transfer by these enzymes (25–30). Magnesium is thought to interact with phosphate groups and to accept and donate protons during catalysis. In a generally accepted transition state in polymerases, a hexacoordinated Mg^{2+} stabilizes the triphosphate of the newly base paired (d)NTP, while a partially hydrated Mg^{2+} activates the 3′-OH of the primer for nucleophilic attack on the 5′-phosphate of the (d)NTP, thereby completing the

*To whom correspondence should be addressed. Tel: +1 404 385 6258; Fax: +1 404 894 7452; Email: loren.williams@chemistry.gatech.edu

Table 1. Mg^{2+} versus Fe^{2+}

	r (Å)[a]	AOCN[b]	$-\Delta H_{hyd}$[c]	pK_a[d]	ΔH[h]
Mg^{2+}	0.65	6	458[e]	11.4	
Fe^{2+}[f]	0.74	6	464[g]	9.5	−1.3

(a) Ionic radius (19); (b) Average Observed Coordination Number (19); (c) Hydration enthalpy (kcal mol^{-1}); (d) pKa of $M^{2+}(H2O)_6$ where $M^{2+} = Fe^{2+}$ or Mg^{2+} (20); (e) From Rashina and Honig (21); (f) High spin; (g) From Uudsemaa and Tamm (22); (h) Relative interaction enthalpy (kcal mol^{-1}) for RNA clamp formation (23).

phosphodiester bond. A similar two metal transition state has been proposed for the last step of phosphodiester bond formation by DNA ligase, whereby one metal stabilizes the phosphates of the temporarily adenylated DNA substrate and another activates the hydroxyl group. Probable metal ligands of polymerases and DNA ligase active sites include protein carboxylates, water molecules, and the non-bridging phosphate oxygens and hydroxyls of nucleic acids. Recent work proposes that a third divalent metal ion may also be essential for catalysis (31).

We use experiments to characterize Fe^{2+}-mediated biochemistry in simulated ancient Earth conditions. We have recreated anoxic, Fe^{2+}-rich conditions (pre-GOE conditions) in the laboratory. We test predictions of the $Fe^{2+} \rightarrow Mg^{2+}$ model by removing Mg^{2+} from three nucleic acid processing proteins, and replacing it with Fe^{2+} in the absence of O_2. We test abilities of a DNA polymerase, an RNA polymerase and a DNA ligase to function using Fe^{2+} as a cofactor in place of Mg^{2+}. Specifically, we substituted Fe^{2+} for Mg^{2+} in a thermostable DNA polymerase (Deep Vent exo-) (32), in T7 RNA polymerase (33) and in T4 DNA ligase (34). The results show that Fe^{2+} can substitute for Mg^{2+} in initiation and elongation by the DNA polymerase, in RNA synthesis from a DNA template by the RNA polymerase, and in the joining of DNA oligonucleotides by the ligase.

In addition, we use calculations to reveal differences in energetics, structures and reactivities of Mg^{2+} and Fe^{2+} complexes. We observe that conformations and geometries of hexa aquo or first shell phosphodiester-complexes are conserved when Fe^{2+} is replaced by Mg^{2+}. Compared to Mg^{2+}, Fe^{2+} more effectively withdraws electrons from first shell ligands, causing increases in the electrophilicity of phosphorus atoms of first shell phosphodiester-complexes. By the same mechanism, compared to Mg^{2+}, Fe^{2+} increases the acidity of first shell water molecules. Therefore, Fe^{2+} is expected to be a more effective cofactor than Mg^{2+}. The combined experimental and computational results are consistent with the $Fe^{2+} \rightarrow Mg^{2+}$ model and suggest that some modern nucleic acid processing enzymes retain latent abilities to revert to primordial Fe^{2+}-based states when exposed to pre-GOE conditions.

MATERIALS AND METHODS

Polymerase chain reactions

Polymerase chain reactions (PCR) was performed in a Coy anaerobic chamber in 20 mM Tris–HCl (pH 8.8), 10 mM KCl, 10 mM $(NH_4)_2SO_4$, 0.1% Triton® X-100, 100 μg/ml nuclease-free bovine serum albumin, 1 mM dNTPs, 500 nM Cy3-labeled reverse primer, 500 nM forward primer, 0.5 nM template, 1 U DeepVent® (exo-) DNA polymerase (New England Biolabs). Reaction solutions contained either 2 mM $MgSO_4$, 2 mM $FeCl_2$, 2 mM $MnCl_2$ or in negative controls, no divalent cations. Master mix solutions were prepared with all components except the polymerase and divalent cation, and lyophilized to dryness. We have previously demonstrated that our protocols remove oxygen from reaction mixtures (23,24). Using these methods there is no observable Fenton degradation of RNA in the presence of Fe^{2+} and Fe^{2+} substitutes for Mg^{2+} in RNA folding and ribozyme catalysis.

The DNA polymerase was added to the dry master mix, which was then transferred into the anaerobic chamber. Divalent cation solutions and nuclease-free H_2O, pre-equilibrated in the anoxic atmosphere, were added to produce four PCR mixtures, one with 2 mM Mg^{2+}, one with 2 mM Fe^{2+}, one with 2 mM Mn^{2+} and one lacking divalent cations. Ten microliter of each PCR solution were aliquoted to eight PCR tubes for a total of 32 reactions. One of these was kept at room temperature and served as a negative PCR control (Reaction 0). Tubes were heated to 95°C for 2 min in a thermal cycler and cycled through 2, 4, 8, 12, 16, 20 or 24 PCR cycles. A cycle consisted of (i) denaturation at 95°C for 30 s, (ii) annealing at 52°C for 30 s and (iii) extension at 72°C for 30 s. Divalent cations were removed from the reaction mixtures by incubation with Bio-Rad Chelex 100 Resin. The resin was removed with 0.22 μm centrifugal filters, rendering the samples stable in the presence O_2. The metal-free solutions were taken out of the anaerobic chamber and diluted 1:10 with nuclease-free water. One microliter of each diluted PCR solution was mixed with 9 μl of 10% glycerol and loaded onto a 12% 19:1 polyacrylamide gel buffered in Tris–Borate-Ethylenediaminetetraacetic acid (EDTA), pH 8.4. The reverse primer was also diluted in 10% glycerol and loaded onto the same gel. Each of the polyacrylamide gels were run at 100 V for 70 min at ambient temperature. Gels were imaged using a General Electric Typhoon Trio+ Imager. PCR template and primer sequences are provided in the Supplementary Information.

In vitro transcription

For *in vitro* transcription reactions, DNA template was generated by digestion of intact plasmid pUC19 containing the *Thermus thermophilus* Domain III rRNA gene (35) with HindIII, overnight, in NEB CutSmart buffer. The enzyme was heat inactivated at 80°C for 20 min and linearized DNA purified with an IBI Scientific Gel/PCR DNA Fragment Extraction kit.

The *in vitro* transcription reactions were performed in a Coy anaerobic chamber. Master mix solutions were pre-

pared with all components except the T7 RNA polymerase and divalent cation, lyophilized to dryness, then introduced to the anaerobic chamber. In the chamber, the master mix was re-suspended in water that had been pre-equilibrated to the chamber atmosphere. Final reaction conditions were 1× RNA polymerase reaction buffer (40 mM Tris–HCl, pH 7.9, 2 mM spermidine, 1 mM dithiothreitol), 0.375 mM each nucleoside triphosphate, 5.4 μM linearized DNA template and 5–6 U NEB T7 RNA Polymerase (cat no. M0251S) per microliter of reaction volume, in addition to variable concentrations of $MgCl_2$, $FeCl_2$ or water (control reactions lacked divalent cations). Reactions were incubated at 37°C for 1 h then quenched with excess EDTA. Quenched reactions were removed from the anoxic chamber, mixed with at least an equal volume of ambion gel loading buffer II (95% formamide, 18 mM EDTA and 0.025% each of sodium dodecylsulphate (SDS), xylene cyanol and bromophenol blue), heated to 95°C for 5 min and loaded onto a 5% denaturing polyacrylamide gel alongside a single stranded RNA marker. Gels were run at 120 V for 1 h 20 min, stained with EtBr and imaged on a GE/Amersham Imager 600.

The supplementary material (Supplementary Figure S1) demonstrates that the intensity of the DNA template band decreases when the transcription reaction is successful and that the intensity of RNA transcription product band increases when the completed reaction mixture is treated with DNase [TURBO DNase (Ambion)]. These changes in band intensities arise because complexes of the DNA template and RNA transcript can be so stable that they survive the denaturing conditions and shift the DNA template out of the primary band on the gel. However, these complexes do not survive DNase treatment and the intensity of the transcript band is increased by DNase treatment. These phenomena are illustrated by a series of controls shown in Supplementary Figure S1 and in Figure 2 of the manuscript (note the three lanes with the *least* amount transcript *appear* to have the *most* template). The topmost band of the gels (Figure 2, Supplementary Figures S1 and S2) contains aggregates and long nucleic acids that do not enter the gel.

Ligase reactions

Ligase reactions were performed in the Coy anaerobic chamber in 50 mM Tris–HCl (pH 7.4), 1 mM adenosine triphosphate and 10 mM dithiothreitol. Two semi-complementary DNA 12-mers, one with 5′-phosphate, were used in the ligation reaction. The sliding half-complementary oligonucleotide sequences were 5′-pGAATGGGTAGAC-3′ and 5′-CCATTCGTCTAC-3′. Seven μM of each oligonucleotide was incubated with 200 U of T4 DNA ligase (New England Biolabs) and 10 mM $MgCl_2$ or 10 mM $FeCl_2$. Negative control experiments lacked divalent cations.

DNA oligonucleotides and a ligase master mix containing all reaction components except divalent cations and ligase were lyophilized to dryness, transferred to the anaerobic chamber, equilibrated with the anoxic atmosphere and dissolved in degassed nuclease-free water. T4 DNA ligase was brought into the chamber and equilibrated with the anoxic atmosphere. Once equilibrated, the ligase was then added to the master mix. The solution was divided into three aliquots. Mg^{2+}, Fe^{2+} or nuclease-free water was added to each of the tubes. The reactions were incubated at room temperature for 1 h. Reactions were terminated by incubation with Bio-Rad Chelex 100 Resin. The resin was removed with 0.22 μm centrifugal filters transferred out of the chamber for analysis. Ten microliter of the filtrate was added to 10 μl of loading dye (47.5% formamide, 0.01% SDS, 0.01% bromophenol blue, 0.005% Xylene Cyanol, 0.5 mM EDTA), followed by heating to 90°C for 5 min and quick cooling on ice for 10 min. Samples were loaded onto a 6% denaturing polyacrylamide gel buffered in tris–borate EDTA, pH 8.4. Gels were run at 100 V for 30 min. at ambient temperature, stained with SYBR Green I and imaged on a General Electric Typhoon Trio+ Imager.

Computation

Hexa aquo complexes $[M^{2+}(H_2O)_6]$ and M^{2+}-RNA clamps (where $M = Fe^{2+}$ or Mg^{2+}) were optimized at the unrestricted B3LYP/6–31G(d,p) level of theory. For Fe^{2+} the spin was two and multiplicity was five. For Mg^{2+}, the spin was zero and the multiplicity was one. Single point energies for these complexes were further obtained at the (U)B3LYP/6–311++G(d,p) level of theory using SCF options DIIS, NOVARACC, VTL and MaxCyc = 1000.

The coordinates of the Mg^{2+}-RNA clamp were extracted from the x-ray structure of the *Haloarcula marismortui* large ribosomal subunit (PDB entry: 1JJ2) (36) as previously described (37). The free 5′ and 3′ termini of the phosphate groups were capped with methyl groups in lieu of the remainder of the RNA polymer, and hydrogen atoms were added where appropriate. An Fe^{2+}-RNA clamp was constructed from the Mg^{2+} clamp by converting Mg^{2+} to Fe^{2+} as described (23). The binding of an Mg^{2+} or Fe^{2+} ion to an RNA fragment is described by the following reaction:

$$RNA^{2-} + M^{2+}(H_2O)_6 \rightarrow RNA^{2-} - M^{2+}(H_2O)_4 + 2H_2O,$$

where, $M^{2+} = Mg^{2+}$ or Fe^{2+}.

The reactants and products of this reaction were fully optimized using the density functional theory with the hybrid B3LYP functional, which combines the generalized gradient approximation (GGA) exchange three-parameter hybrid functional of Becke (38) and the correlation functional of Lee-Yang-Parr (39), with the 6–311++G(d,p) basis set as implemented in Gaussian 09 (40).

Natural Bond Order (NBO) (41) and natural energy decomposition analysis (NEDA) (41,42) were performed on the optimized complexes at the (U)B3LYP/6–31G(d,p) level of theory using the GAMESS package (43) and the NBO 5.0 routine. For NEDA calculations, metal-phosphate clamps were treated as products and the free sugar-phosphate backbones and hexa aquo metals were reactants.

RESULTS

We have investigated the ability of a DNA polymerase, an RNA polymerase and a DNA ligase to function using Fe^{2+} instead of Mg^{2+} as a cofactor under simulated ancient earth conditions. All reactions were performed in a Coy anaerobic chamber in an atmosphere of 95% argon and 5% hydro-

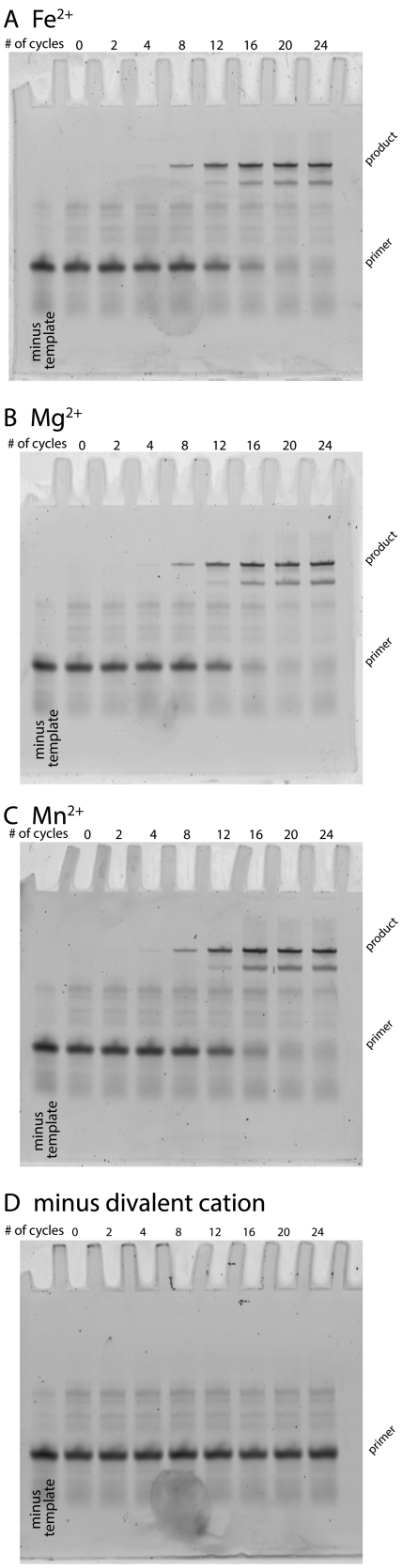

Figure 1. Fe^{2+} or Mn^{2+} can replace Mg^{2+} as a cofactor for Deep Vent (exo-) DNA polymerase. Reaction mixtures with Fe^{2+} or Mg^{2+} or Mn^{2+} or no divalent cation were analyzed for amount of reactants and products at every other PCR cycle for 24 cycles. Reactant consumption and product yields are identical within the uncertainty of this experiment among (**A**) Fe^{2+}, (**B**) Mg^{2+} or (**C**) Mn^{2+}. (**D**) The divalent-minus controls, which lack divalent cations, did not generate product. Neither did the 'minus template' negative control reactions (far left lanes of each gel), taken through 24 cycles, generate product.

gen. Each reaction was run multiple times to ensure reproducibility.

DNA polymerase

Fe^{2+} substitutes for Mg^{2+} as a cofactor for DNA polymerase. We have investigated polymerization using Deep Vent (exo-) DNA polymerase. We used PCR in the presence of Mg^{2+} or Fe^{2+} or Mn^{2+} or in the absence of divalent cations to amplify a 72 nucleotide DNA fragment. Mg^{2+}, Fe^{2+} and Mn^{2+} each facilitate formation of polymerization product. We determined the amount of reactants (primers) and product in the reaction mixture at every other PCR cycle (Figure 1). For divalent cations Mg^{2+} or Fe^{2+} or Mn^{2+}, reaction product is first visible on the gel at cycle eight. The primer is fully consumed in all reactions by cycle twenty. It can be seen that these three divalent cations produce identical yields under the conditions of the reaction within the error of the experiment. If the yields were not similar for each divalent cation at each cycle, the cycle numbers at which primer disappears and at which product appears would vary between the different divalent cations. The absence of product in the reaction lacking divalent cations demonstrates that Mg^{2+} extraction methods are efficient and that the product observed in the Fe^{2+} reaction is not attributable to contaminating Mg^{2+}.

RNA polymerase

Fe^{2+} substitutes for Mg^{2+} as a cofactor for T7 RNA polymerase. Digested plasmid encoding a template for a 376 nucleotide fragment of Domain III rRNA (44) was used with varying concentrations of Mg^{2+} or Fe^{2+}. Full length RNA product is observed at all concentrations of Mg^{2+} investigated here, and at concentrations of Fe^{2+} up to 6 mM (Figure 2). No RNA product is observed in control reactions without added divalent metals, confirming that the RNA products in the Fe^{2+} reactions do not result from Mg^{2+} contamination. The divalent cation concentration that gives a maximum RNA yield is less for Fe^{2+} than for Mg^{2+}. At 0.75 mM of either divalent cation, the product yield is greater for Fe^{2+} than for Mg^{2+}. Therefore, at low divalent metal concentrations T7 RNA polymerase appears more active in the presence of Fe^{2+} than in Mg^{2+}. These experiments were independently replicated, giving consistent results in each replica. The identities of other bands on the gels are discussed in 'Materials and Methods' section and Supplementary Figure S1.

The Mg^{2+} optimum for T7 DNA polymerase is around 10 mM, depending on the presence of other cations (45). The concentration optimum is an order of magnitude lower for Fe^{2+} than for Mg^{2+}. Under the conditions of these reac-

Table 2. Interaction energies in RNA/DNA clamps of Fe^{2+} and Mg^{2+}

Complex	E(kcal/mol)[a][kcal/mol][a]
RNA^{2-}–$Mg(H_2O)_4^{2+}$ [b]	−31.9
DNA^{2-}–$Mg(H_2O)_4^{2+}$ [b]	−20.4
RNA^{2-}–$Fe(H_2O)_4^{2+}$	−43.7
DNA^{2-}–$Fe(H_2O)_4^{2+}$	−25.4

(a) with basis set superposition error in aqueous phase.
(b) from Petrov (37).

tions, the T7 RNA polymerase yield decreases with increasing Fe^{2+}. At 60 mM Fe^{2+} the yield drops to zero (Supplementary Figure S2).

DNA ligase

We have investigated a ligation reaction using sliding-half complementary DNA oligonucleotides ('Materials and Methods' section). The oligonucleotides were ligated using T4 DNA ligase in the presence of either Mg^{2+}or Fe^{2+} and in the absence of divalent cations. The results demonstrate that T4 DNA ligase is functional with either Mg^{2+} or Fe^{2+}. The Fe^{2+} reaction forms less product and shorter fragments than the Mg^{2+} reaction. We observe ligation products up to 14 substrates in length with T4 ligase in the presence of Mg^{2+}, and ligation products seven substrates in length in the presence of Fe^{2+} (Figure 3). On the gel, each successive band of increasing DNA length corresponds to an increase in product length by the ligation of one additional oligonucleotide. The absence of significant product in the control reaction confirms that the product observed in the Fe^{2+} reaction is not be attributed to contaminating Mg^{2+}.

Computation

The geometries of RNA^{2-}–$Fe^{2+}(H_2O)_4$ and RNA^{2-}–$Mg^{2+}(H_2O)_4$ clamps (37) and of hexa aquo Fe^{2+} and hexa aquo Mg^{2+} were optimized. Each clamp consists of a (deoxy)ribose with 5′ and 3′ phosphates and four water molecules. M^{2+} is six-coordinate in all complexes.

The conformations of RNA clamps are nearly identical with Fe^{2+} and Mg^{2+}, with very similar metal-ligand distances (Supplementary Table S1). The average metal to oxygen (water) distance is 2.16 Å for Mg^{2+} and 2.15 for Fe^{2+}. The interaction energies are also similar between Fe^{2+} and Mg^{2+}, although the Fe^{2+} clamp is slightly more stable than the Mg^{2+} clamp (Table 2) due to charge transfer to the vacant d-orbitals of Fe^{2+} (Figure 4, Supplementary Tables S2 and 3). RNA and DNA clamp more tightly to either Fe^{2+} or Mg^{2+} than to Na^+ or Ca^{2+} (37). RNA clamps are more stable than DNA clamps.

Hexa aquo complexes. The calculations show why hexa aquo Fe^{2+} is a stronger acid than hexa aquo Mg^{2+}. Fe^{2+} confers greater positive charge on its first shell waters than Mg^{2+}. In comparison with Mg^{2+}, Fe^{2+} withdraws 0.142 more electrons from its first shell water molecules (Supplementary Tables S4 and S5). The net charge on Fe^{2+} in a hexa aquo complex is +1.631 while the net charge on Mg^{2+} in a hexa aquo complex is +1.773. The calculations show that 0.369 electrons are transferred from the six first shell water molecules to Fe^{2+}, while only 0.227 electrons are transferred to Mg^{2+}. The net number of electrons transferred from the average first shell water of hexa aquo Fe^{2+} is 0.060 electrons per water molecule. The net number of electrons transferred from the average first shell water of hexa aquo Mg^{2+} is 0.037 electrons per water molecule.

DISCUSSION

Here we recapitulate the reductive potential of the Archean atmosphere (46–48). Kasting's high CO_2 model of the Archean atmosphere (46) has been re-evaluated (48); geological data is considered to be incompatible with this model (47,49). Although the specific chemical composition of the Archean atmosphere remains unresolved, it is accepted that it was reductive and that the biosphere was iron-rich and was lacking O_2. Life originated and first proliferated in a reductive iron-rich environment, which persisted until around 2 billion years ago, when the GOE began depleting iron from the biosphere (1–4,23) and fostering Fe^{2+}/O_2 mediated cellular damage (7).

The environment of the ancient Earth is consistent with a $Fe^{2+} \rightarrow Mg^{2+}$ model in which Fe^{2+} was an important cofactor for both nucleic acids and proteins during early evolution. Extant protein enzymes process nucleic acids using Mg^{2+} as a cofactor but might have used Fe^{2+} on the early earth. It is possible that extant biopolymers retain intrinsic adaptation to Fe^{2+}. Indeed, previous experimental substitution of Fe^{2+} for Mg^{2+} in association with RNA demonstrated that Fe^{2+} can facilitate RNA folding and expand RNA catalytic breadth (23,24).

To determine if the $Fe^{2+} \rightarrow Mg^{2+}$ model is plausible, and if ancient nucleic acid processing enzymes might have used Fe^{2+} instead of Mg^{2+} as a primary cofactor, here we substituted Fe^{2+} for Mg^{2+} in a DNA polymerase, an RNA polymerase and a DNA ligase. Polynucleotide polymerases are ubiquitous enzymes that perform some of the most critical and universal enzymatic activities in the biological world. Polymerases synthesize polynucleotides from (d)NTPs by covalently joining nucleotides as directed by a template. Polymerases use di-metal centers with metals coordinated by the protein and during catalysis, by phosphate groups of the substrate (25). The di-metal centers in DNA and RNA polymerases are thought to (i) stabilize a pentacovalent transition state, (ii) facilitate the leaving of pyrophosphate and (iii) lower the pKa of the 3′-hydroxyl of the terminus. Mg^{2+} is the thought to be the preferred divalent ion *in vivo* for polymerases. The results here demonstrate that Fe^{2+}, in a reductive environment, can substitute for Mg^{2+} in function of both DNA and RNA polymerases. It was shown previously that Mn^{2+} (50,51), or with reduced functionality, Ca^{2+} (52), can substitute for Mg^{2+} in some polymerases *in vitro*.

DNA ligase, another ancient protein enzyme, is required for DNA replication and repair (34,53). DNA ligase catalyzes the joining of terminal 5′-phosphoryl and 3′-hydroxyl groups of DNA fragments. DNA ligase joins Okazaki fragments produced by lagging strand DNA synthesis and seals nicks after DNA excision repair. Ligation uses three sequential nucleotidyl transfers, each of which requires a divalent

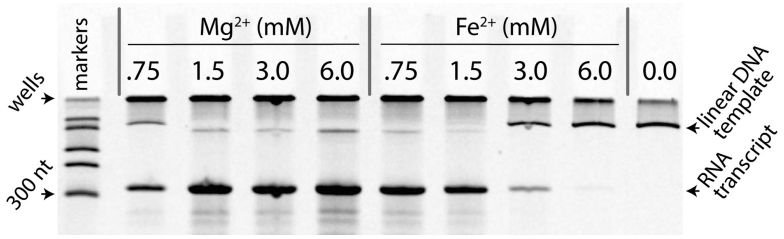

Figure 2. Fe^{2+} can replace Mg^{2+} as a cofactor in transcription by T7 RNA polymerase. Full length RNA transcript is observed with either Mg^{2+} or Fe^{2+}. No product is observed in the no-divalent negative control. The far left lane contains ssRNA size markers. The top of the gel contains large and/or aggregated nucleic acids that remain in the wells during electrophoresis.

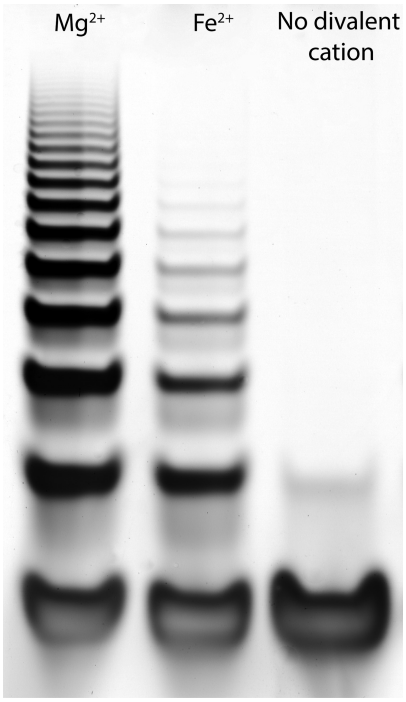

Figure 3. Fe^{2+} can replace Mg^{2+} as a cofactor for T4 DNA ligase. Ligation products of sliding-half complementary oligonucleotides are observed with both Mg^{2+} and Fe^{2+}. No product is observed in the divalent-minus negative control. See 'Materials and Methods' section for oligonucleotide sequences.

metal cofactor. Mg^{2+} is thought to be the preferred ion *in vivo*. A ferric iron-containing ligase with an exceptionally low pH optimum has been isolated from an acidophilic ferrous iron-oxidizing archaeon (54). Structural and possibly catalytic roles for the ferric iron are possible. Unlike the systems we investigate here, the ferric ligase is not active in the presence of Mg^{2+}.

Like DNA and RNA polymerases, DNA ligases are believed to contain di-metal centers within their active sites. Metals are coordinated by the protein and, during catalysis, by substrate phosphate groups (34,53). The di-metal center activates hydroxyl groups for nucleophilic attack and stabilizes leaving groups. The results here indicate that Fe^{2+} can substitute for Mg^{2+} in a ligase di-metal center. In the presence of Fe^{2+}, the ligase is functional but may be less active than in the presence of Mg^{2+}.

Mechanisms of phosphoryl transfer and geometries of di-metal centers are highly conserved and thought to be evolutionarily ancient (25). Formation of di-metal centers appears to be required for activity of the enzymes investigated here. Therefore, it appears functional di-iron centers form in DNA and RNA polymerases and in DNA ligases under our experimental conditions. The facility of substitution of Fe^{2+} for Mg^{2+} demonstrated here suggests that di-metal centers, including di-iron centers in enzymes such as ribonucleotide reductase (15) and di-magnesium centers in polymerases (25,55) and in large RNAs (56), may be related by common ancestry or by origins in a common chemical environment. Observed activity of polynucleotide polymerases and a DNA ligase in the presence of Fe^{2+} is consistent with similar coordination geometries and chemistries between Mg^{2+} and Fe^{2+} (Table 1). However, decreased activity of these enzymes in the presence of Fe^{+2} instead of Mg^{2+} might be expected after nearly 2 billion years of evolution that would have optimized the use of Mg^{2+} as a cofactor, rather than Fe^{2+}.

Although Mg^{2+} and Fe^{2+} are characterized by similar coordination geometries and chemistries (Table 1), and can substitute for each other in di-metal centers, they are distinguished by important differences. We have observed that Fe^{2+} can be a more potent cofactor than Mg^{2+} in RNA folding. RNA folds at lower concentrations of Fe^{2+} than Mg^{2+}, and that at least a subset of ribozymes are more active in Fe^{2+} than in Mg^{2+} (23). In addition, we observe here that at low concentrations of divalent cations, T7 RNA polymerase is more active in the presence of Fe^{2+} than Mg^{2+}. To attempt to understand the origins of these differences, we have used computation to determine the effects of substitution of Fe^{2+} for Mg^{2+} in hexa aquo complexes and in complexes with first shell phosphodiester ligands.

We have modeled phosphate complexes of Fe^{2+} and Mg^{2+}. The results allow us to understand the roles of divalent cations in RNA folding and during important catalytic steps of polymerization and ligation reactions. The forces, energetics and electronic perturbations within phosphate complexes of Fe^{2+} and Mg^{2+}complexes were characterized by density functional methods (57–63). Components of the interaction energy, such as charge transfer, polarization and exchange were investigated with NBO and NEDA (41,42). The computations reveal subtle yet critical differences between Mg^{2+} and Fe^{2+}.

Computation helps explain why Fe^{2+} can be a potent cofactor for nucleic acid processing enzymes. Conformations

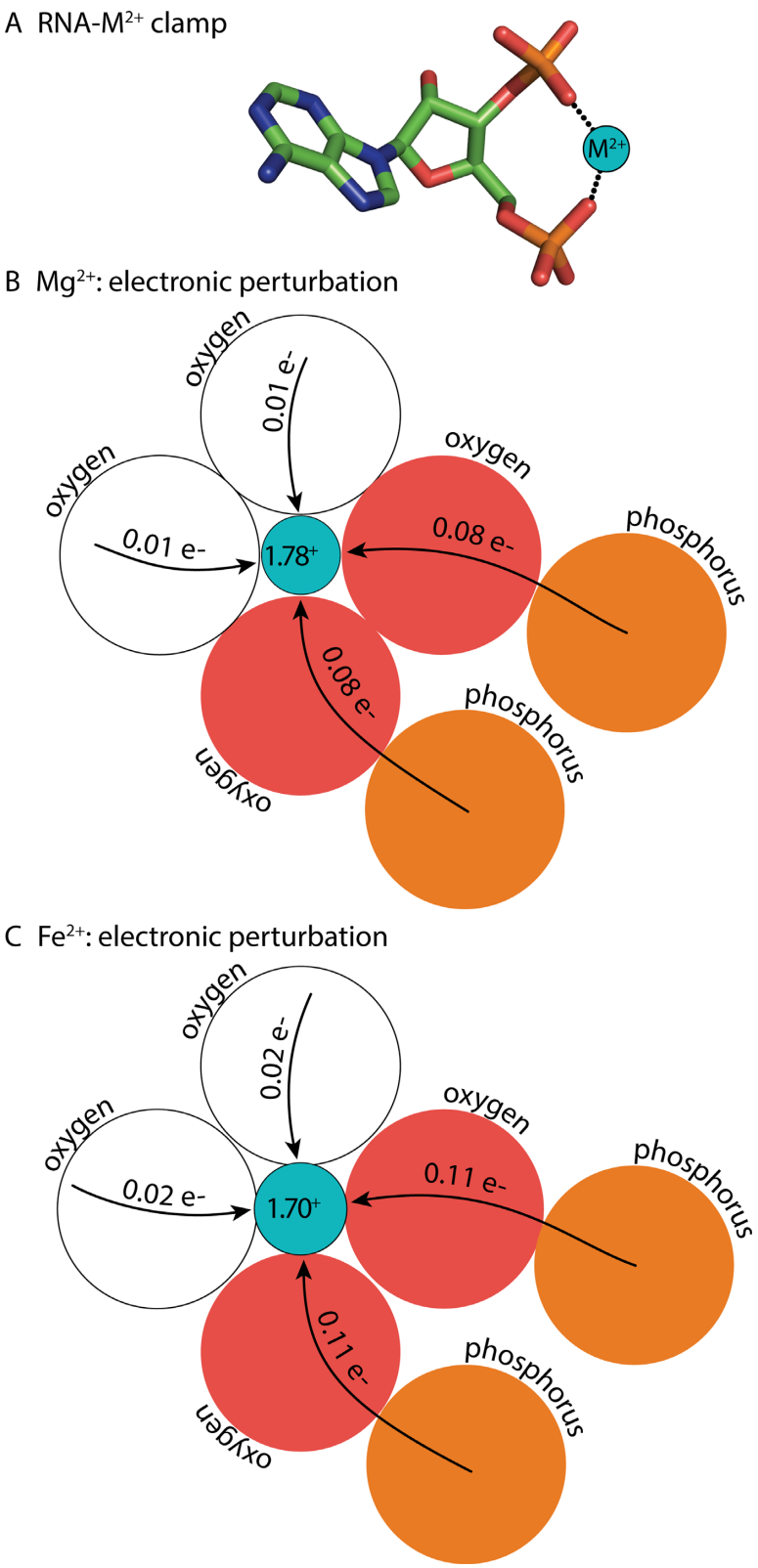

Figure 4. (**A**) A three-dimensional representation of a common M^{2+} complex in RNA in which the M^{2+} ion is coordinated directly by two phosphate oxygens in an RNA-M^{2+} clamp. The M^{2+} is six coordinate; the four first shell water molecules are omitted for clarity. (**B**) Electronic schematic of the M^{2+} complex shown in panel A where $M^{2+} = Mg^{2+}$. The two axial water oxygen atoms are omitted for clarity. (**C**) Electronic schematic of the M^{2+} complex shown in panel A where $M^{2+} = Fe^{2+}$. The atoms are labeled in all three panels.

and geometries are nearly identical between complexes of Fe^{2+} or Mg^{2+}. These similarities are observed in both hexa aquo and phosphate complexes. Important differences between Mg^{2+} and Fe^{2+} follow. (i) Interactions with water. Hexa aquo Fe^{2+} is a stronger acid than hexa aquo Mg^{2+} (Table 1). Our calculations show greater depletion of electrons from water molecules that coordinate Fe^{2+} than those that coordinate Mg^{2+}. Greater frequency of $M^{2+}(H_2O)_5(OH^-)$ as predicted for Fe^{2+} over Mg^{2+} would facilitate important reactions in which a ribose hydroxyl gives up a proton while acting as a nucleophile. (ii) Nucleophilic attack at phosphorus. Because of low lying d orbitals, Fe^{2+} has greater electron withdrawing power than Mg^{2+} from first shell phosphate ligands (Figure 4, Supplementary Tables S2 and 3). In coordination complexes with phosphate groups, the phosphorus atom is a better electrophile when $M^{2+} = Fe^{2+}$ than when $M^{2+} = Mg^{2+}$. Modulation of rates of nucleophilic attack on phosphorus is important in many biological reactions, including formation of phosphodiester bonds in polymerization and ligation. This difference between Mg^{2+} and Fe^{2+} is apparent in ribozyme reactions. We have observed that phosphoryl transfer ribozymes, including a ribozyme selected in the presence of Mg^{2+}, are more active with Fe^{2+} as a cofactor than with Mg^{2+} (23). (iii) Phosphate affinity. Also because of low-lying d orbitals, Fe^{2+} interacts with slightly greater affinity than Mg^{2+} with the oxygen atoms of first shell phosphate ligands. Tighter binding of M^{2+} to RNA appears to improve folding and would be important during the catalytic reactions assayed here.

CONCLUSION

Popović and Ditzler performed what was, to our knowledge, the first-ever *in vitro* RNA selection under plausible pre-GOE conditions (64) and demonstrated that ribozymes obtained by selection with Fe^{2+} are active upon substitution of Mg^{2+} for Fe^{2+}. Here we begin to test the hypothesis that Fe^{2+} was a divalent cation that actively facilitated processing of nucleic acids by proteins on the ancient Earth. We have investigated ancient Earth biochemistry of proteins that play important roles in nucleic acid processing. Polymerases and ligases are both important in DNA replication, RNA transcription and DNA repair. The ability of Fe^{2+} to substitute for Mg^{2+} in the polymerases and the ligase suggests that Fe^{2+}, in the absence of O_2, could substitute for Mg^{2+} in a broad variety of enzymes involved in nucleic acid processing. We have used calculations to show that Fe^{2+} is a viable substitute for Mg^{2+} in nucleic acid-cation interactions. Therefore, Fe^{2+} might have played a role in the early evolution of proteins and nucleic acids.

SUPPLEMENTARY DATA

Supplementary Data are available at NAR Online.

FUNDING

National Aeronautics and Space Administration [NNX16AJ28G, in part]. Funding for open access charge: NASA [NNX16J28G].
Conflict of interest statement. None declared.

REFERENCES

1. Hazen,R.M. and Ferry,J.M. (2010) Mineral evolution: mineralogy in the fourth dimension. *Elements*, **6**, 9–12.
2. Anbar,A.D. (2008) Oceans. elements and evolution. *Science*, **322**, 1481–1483.
3. Holland,H.D. (2006) The oxygenation of the atmosphere and oceans. *Philos. Trans. R. Soc. Lond. B Biol. Sci.*, **361**, 903–915.
4. Klein,C. (2005) Some precambrian banded iron-formations (BIFs) from around the world: their age, geologic setting, mineralogy, metamorphism, geochemistry, and origin. *Am. Mineral.*, **90**, 1473–1499.
5. Holland,H.D. (1973) The oceans: a possible source of iron in iron-formations. *Econ. Geol.*, **68**, 1169–1172.
6. Kozlowski,H., Kolkowska,P., Watly,J., Krzywoszynska,K. and Potocki,S. (2014) General aspects of metal toxicity. *Curr. Med. Chem.*, **21**, 3721–3740.
7. Prousek,J. (2007) Fenton chemistry in biology and medicine. *Pure Appl. Chem.*, **79**, 2325–2338.
8. Harel,A., Bromberg,Y., Falkowski,P.G. and Bhattacharya,D. (2014) Evolutionary history of redox metal-binding domains across the tree of life. *Proc. Natl. Acad. Sci. U.S.A.*, **111**, 7042–7047.
9. Dupont,C.L., Yang,S., Palenik,B. and Bourne,P.E. (2006) Modern proteomes contain putative imprints of ancient shifts in trace metal geochemistry. *Proc. Natl. Acad. Sci. U.S.A.*, **103**, 17822–17827.
10. Theil,E.C. and Goss,D.J. (2009) Living with iron (and oxygen): questions and answers about iron homeostasis. *Chem. Rev.*, **109**, 4568–4579.
11. Valko,M., Morris,H. and Cronin,M.T.D. (2005) Metals, toxicity and oxidative stress. *Curr. Med. Chem.*, **12**, 1161–1208.
12. Aguirre,J.D. and Culotta,V.C. (2012) Battles with iron: manganese in oxidative stress protection. *J. Biol. Chem.*, **287**, 13541–13548.
13. Ushizaka,S., Kuma,K. and Suzuki,K. (2011) Effects of Mn and Fe on growth of a coastal marine diatom talassiosira weissflogii in the presence of precipitated Fe(III) hydroxide and EDTA-Fe(III) complex. *Fish. Sci.*, **77**, 411–424.
14. Martin,J.E. and Imlay,J.A. (2011) The Alternative aerobic ribonucleotide reductase of *Escherichia Coli*, NrdEF, is a manganese-dependent enzyme that enables cell replication during periods of iron starvation. *Mol. Microbiol.*, **80**, 319–334.
15. Cotruvo,J.A. and Stubbe,J. (2011) Class I ribonucleotide reductases: metallocofactor assembly and repair in vitro and in vivo. *Annu. Rev. Biochem.*, **80**, 733–767.
16. Anjem,A., Varghese,S. and Imlay,J.A. (2009) Manganese import is a key element of the oxyr response to hydrogen peroxide in *Escherichia Coli*. *Mol. Microbiol.*, **72**, 844–858.
17. Wolfe-Simon,F., Starovoytov,V., Reinfelder,J.R., Schofield,O. and Falkowski,P.G. (2006) Localization and role of manganese superoxide dismutase in a marine diatom. *Plant Physiol.*, **142**, 1701–1709.
18. Torrents,E., Aloy,P., Gibert,I. and Rodriguez-Trelles,F. (2002) Ribonucleotide reductases: divergent evolution of an ancient enzyme. *J. Mol. Evol.*, **55**, 138–152.
19. Brown,I.D. (1988) What factors determine cation coordination numbers? *Acta Crystallogr. Sect. B.*, **44**, 545–553.
20. Wulfsberg,G. (1991) *Principles of descriptive inorganic chemistry*. University Science Books, Sausalito.
21. Rashin,A.A. and Honig,B. (1985) Reevaluation of the born model of ion hydration. *J. Phys. Chem.*, **89**, 5588–5593.
22. Uudsemaa,M. and Tamm,T. (2004) Calculation of hydration enthalpies of aqueous transition metal cations using two coordination shells and central ion substitution. *Chem. Phys. Lett.*, **400**, 54–58.
23. Athavale,S.S., Petrov,A.S., Hsiao,C., Watkins,D., Prickett,C.D., Gossett,J.J., Lie,L., Bowman,J.C., O'Neill,E., Bernier,C.R. *et al.* (2012) RNA folding and catalysis mediated by iron (II). *PLoS One*, **7**, e38024.
24. Hsiao,C., Chou,I.-C., Okafor,C.D., Bowman,J.C., O'Neill,E.B., Athavale,S.S., Petrov,A.S., Hud,N.V., Wartell,R.M., Harvey,S.C. *et al.* (2013) Iron(II) plus RNA can catalyze electron transfer. *Nat. Chem.*, **5**, 525–528.
25. Steitz,T.A. (1999) DNA polymerases: structural diversity and common mechanisms. *J. Biol. Chem.*, **274**, 17395–17398.
26. Doherty,A.J. and Dafforn,T.R. (2000) Nick recognition by DNA ligases. *J. Mol. Biol.*, **296**, 43–56.

27. Lee,J.Y., Chang,C., Song,H.K., Moon,J., Yang,J.K., Kim,H.K., Kwon,S.T. and Suh,S.W. (2000) Crystal structure of nad+-dependent DNA ligase: modular architecture and functional implications. *EMBO J.*, **19**, 1119–1129.
28. Ellenberger,T. and Tomkinson,A.E. (2008) Eukaryotic DNA ligases: structural and functional insights. *Annu. Rev. Biochem*, **77**, 313–338.
29. Lykke-Andersen,J. and Christiansen,J. (1998) The C-Terminal carboxy group of T7 RNA polymerase ensures efficient magnesium ion-dependent catalysis. *Nucleic Acids Res.*, **26**, 5630–5635.
30. Yin,Y.W. and Steitz,T.A. (2004) The Structural mechanism of translocation and helicase activity in T7 RNA polymerase. *Cell*, **116**, 393–404.
31. Gao,Y. and Yang,W. (2016) Capture of a third Mg^{2+} is essential for catalyzing dna synthesis. *Science*, **352**, 1334–1337.
32. Jannasch,H.W., Wirsen,C.O., Molyneaux,S.J. and Langworthy,T.A. (1992) Comparative physiological studies on hyperthermophilic archaea isolated from deep-sea hot vents with emphasis on pyrococcus strain Gb-D. *Appl. Environ. Microbiol.*, **58**, 3472–3481.
33. Sousa,R. and Mukherjee,S. (2003) T7 RNA polymerase. *Prog. Nucleic Acid Res. Mol. Biol.*, **73**, 1–41.
34. Shuman,S. (2009) DNA ligases: progress and prospects. *J. Biol. Chem.*, **284**, 17365–17369.
35. Athavale,S.S., Gossett,J.J., Hsiao,C., Bowman,J.C., O'Neill,E., Hershkovitz,E., Preeprem,T., Hud,N.V., Wartell,R.M., Harvey,S.C. *et al.* (2012) Domain III of the *T. thermophilus* 23S rRNA folds independently to a near-native state. *RNA*, **18**, 752–758.
36. Ban,N., Beckmann,R., Cate,J.H., Dinman,J.D., Dragon,F., Ellis,S.R., Lafontaine,D.L., Lindahl,L., Liljas,A., Lipton,J.M. *et al.* (2014) A New system for naming ribosomal proteins. *Curr. Opin. Struct. Biol.*, **24**, 165–169.
37. Petrov,A.S., Bowman,J.C., Harvey,S.C. and Williams,L.D. (2011) Bidentate RNA-magnesium clamps: on the origin of the special role of magnesium in RNA folding. *RNA*, **17**, 291–297.
38. Becke,A.D. (1988) Density-functional exchange-energy approximation with correct asymptotic behavior. *Phys. Rev. A*, **38**, 3098–3100.
39. Lee,C.T., Yang,W.T. and Parr,R.G. (1988) Development of the colle-salvetti correlation energy formula into a functional of the electron density. *Phys. Rev. B Condens. Matter*, **37**, 785–789.
40. Frisch,M.J., Trucks,G.W., Schlegel,H.B., Scuseria,G.E., Robb,M.A., Cheeseman,J.R., Scalmani,G., Barone,V., Mennucci,B., Petersson,G.A. *et al.* (2009) *Gaussian 09, Revision A.0.1*. Gaussian, Inc., Wallingford.
41. Glendening,E.D. and Feller,D. (1996) Dication-water interactions: $M^{2+}(H2o)_N$ clusters for alkaline earth metals M=Mg,Ca,Sr,Ba, and Ra. *J. Phys. Chem.*, **100**, 4790–4797.
42. Schenter,G.K. and Glendening,E.D. (1996) Natural energy decomposition analysis: the linear response electrical self energy. *J. Phys. Chem.*, **100**, 17152–17156.
43. Gordon,M.S. and Schmidt,M.W. (2005) Advances in electronic structure theory: GAMESS a decade later. In: Dykstra,CE, Frenking,G, Kim,KS and Scuseria,GE (eds). *Theory and Applications of Computational Chemistry: the First Forty Years*. Elsevier science, Amsterdam, pp. 1167–1189.
44. Lanier,K.A., Athavale,S.S., Petrov,A.S., Wartell,R. and Williams,L.D. (2016) Imprint of ancient evolution on rRNA folding. *Biochemistry*, **55**, 4603–4613.
45. Fuchs,E. (1976) The interdependence of magnesium with spermidine and phosphoenolpyruvate in an enzyme-synthesizing system in vitro. *FEBS J.*, **63**, 15–22.
46. Kasting,J.F. (1987) Theoretical constraints on oxygen and carbon dioxide concentrations in the precambrian atmosphere. *Precambrian Res.*, **34**, 205–229.
47. Ueno,Y., Johnson,M.S., Danielache,S.O., Eskebjerg,C., Pandey,A. and Yoshida,N. (2009) Geological sulfur isotopes indicate elevated ocs in the archean atmosphere, solving faint young sun paradox. *Proc. Natl. Acad. Sci. U.S.A.*, **106**, 14784–14789.
48. Kasting,J.F. and Siefert,J.L. (2002) Life and the evolution of earth's atmosphere. *Science*, **296**, 1066–1068.
49. Rosing,M.T., Bird,D.K., Sleep,N.H. and Bjerrum,C.J. (2010) No climate paradox under the faint early sun. *Nature*, **464**, 744–747.
50. Tabor,S. and Richardson,C.C. (1989) Effect of manganese ions on the incorporation of dideoxynucleotides by bacteriophage T7 DNA polymerase and *Escherichia Coli* DNA polymerase I. *Proc. Natl. Acad. Sci. U.S.A.*, **86**, 4076–4080.
51. Litman,R.M. (1971) The differential effect of magnesium and manganese ions on the synthesis of poly (Dg-Dc) and micrococcus luteus DNA by *Micrococcus Luteus* DNA polymerase. *J. Mol. Biol.*, **61**, 1–23.
52. Irimia,A., Zang,H., Loukachevitch,L.V., Eoff,R.L., Guengerich,F.P. and Egli,M. (2006) Calcium is a cofactor of polymerization but inhibits pyrophosphorolysis by the *Sulfolobus Solfataricus* DNA polymerase Dpo4. *Biochemistry*, **45**, 5949–5956.
53. Subramanya,H.S., Doherty,A.J., Ashford,S.R. and Wigley,D.B. (1996) Crystal structure of an ATP-dependent DNA ligase from bacteriophage T7. *Cell*, **85**, 607–615.
54. Ferrer,M., Golyshina,O.V., Beloqui,A., Böttger,L.H., Andreu,J.M., Polaina,J., De Lacey,A.L., Trautwein,A.X., Timmis,K.N. and Golyshin,P.N. (2008) A purple acidophilic di-ferric DNA ligase from ferroplasma. *Proc. Natl. Acad. Sci. U.S.A.*, **105**, 8878–8883.
55. Steitz,T.A. and Steitz,J.A. (1993) A general two-metal-ion mechanism for catalytic RNA. *Proc. Natl. Acad. Sci. U.S.A.*. **90**, 6498–6502.
56. Hsiao,C. and Williams,L.D. (2009) A recurrent magnesium-binding motif provides a framework for the ribosomal peptidyl transferase center. *Nucleic Acids Res.*, **37**, 3134–3142.
57. Rulisek,L. and Sponer,J. (2003) Outer-shell and inner-shell coordination of phosphate group to hydrated metal ions (Mg^{2+}, Cu^{2+}, Zn^{2+}, Cd^{2+}) in the presence and absence of nucleobase. The role of nonelectrostatic effects. *J. Phys. Chem. B*, **107**, 1913–1923.
58. Gresh,N., Sponer,J.E., Spackova,N., Leszczynski,J. and Sponer,J. (2003) Theoretical study of binding of hydrated Zn(II) and Mg(II) cations to 5′-guanosine monophosphate. Toward polarizable molecular mechanics for DNA and RNA. *J. Phys. Chem. B*, **107**, 8669–8681.
59. Munoz,J., Sponer,J., Hobza,P., Orozco,M. and Luque,F.J. (2001) Interactions of hydrated Mg^{2+} cation with bases, base pairs, and nucleotides. Electron topology, natural bond orbital, electrostatic, and vibrational study. *J. Phys. Chem. B*, **105**, 6051–6060.
60. Trachtman,M., Markham,G.D., Glusker,J.P., George,P. and Bock,C.W. (1998) Interactions of metal ions with water: Ab initio molecular orbital studies of structure, bonding enthalpies, vibrational frequencies and charge distributions. 1. Monohydrates. *Inorg. Chem.*, **37**, 4421–4431.
61. Murashov,V.V. and Leszczynski,J. (1999) Theoretical study of complexation of phosphodiester linkage with alkali and alkaline-earth cations. *J. Phys. Chem. B*, **103**, 8391–8397.
62. Petrov,A.S., Lamm,G. and Pack,G.R. (2005) Calculation of the binding free energy for magnesium-RNA interactions. *Biopolymers*, **77**, 137–154.
63. Petrov,A.S., Pack,G.R. and Lamm,G. (2004) Calculations of magnesium-nucleic acid site binding in solution. *J. Phys. Chem. B*, **108**, 6072–6081.
64. Popović,M., Fliss,P.S. and Ditzler,M.A. (2015) *In vitro* evolution of distinct self-cleaving ribozymes in diverse environments. *Nucleic Acids Res.*, **43**, 7070–7082.